



## Article

# Modeling the Influence of the Electrolyte Concentration on Electrical Characteristics of an Alkaline Electrolyzer

Krzysztof Górecki \* , Emilian Świtalski and Paweł Górecki 

Department of Marine Electronics, Gdynia Maritime University, 81-225 Gdynia, Poland

\* Correspondence: k.gorecki@we.umg.edu.pl

**Abstract:** This paper presents the results of investigations into modeling the DC and dynamic characteristics of an alkaline electrolyzer. A model of the device under consideration is proposed in the form of analytical relationships in which the coefficients depend on the concentration of the potassium hydroxide solution contained in the electrolyzer under consideration. The correctness of the proposed model is verified by comparing the calculated and measured current–voltage characteristics and the dependence of the module of the impedance of the electrolyzer on the frequency obtained at different values of the electrolyte concentration. The dependence of the time needed to produce a given portion of hydrogen on the supply current and the electrolyte concentration is also presented. Good compliance with the calculation and measurement results is obtained over a wide range of voltage and current, frequency, and concentration of the electrolyte.

**Keywords:** alkaline electrolyzer; modelling; SPICE; DC characteristics; AC characteristics; measurements; hydrogen



**Citation:** Górecki, K.; Świtalski, E.; Górecki, P. Modeling the Influence of the Electrolyte Concentration on the Electrical Characteristics of an Alkaline Electrolyzer. *Energies* **2022**, *15*, 8090. <https://doi.org/10.3390/en15218090>

Academic Editor: Muhammad Aziz

Received: 26 September 2022

Accepted: 25 October 2022

Published: 31 October 2022

**Publisher's Note:** MDPI stays neutral with regard to jurisdictional claims in published maps and institutional affiliations.



**Copyright:** © 2022 by the authors. Licensee MDPI, Basel, Switzerland. This article is an open access article distributed under the terms and conditions of the Creative Commons Attribution (CC BY) license (<https://creativecommons.org/licenses/by/4.0/>).

## 1. Introduction

Hydrogen is now seen as the fuel of the future to generate electrical energy to drive vehicles [1] without polluting the environment. This gas can also be used to store an excess of electrical energy generated by renewable power sources [2], such as photovoltaics and wind farms [3]. Using hydrogen technologies, we can produce electrical (fuel cell) or thermal (burners) energy [4–6] at possibly low emission of carbon dioxide (CO<sub>2</sub>) into the atmosphere. This is possible due to, among other things, the use of leaning technologies applied in the reaction of oxygenation of hydrogen.

The European Road Map of production and distribution of hydrogen, fuel cells, and hydrogen systems quoted in the paper [7] in Europe will have changed from the leaning economy of mineral fuels into the leaning economy of hydrogen by the year 2050. Hydrogen can be produced using various methods described, inter alia, in the paper [8]. These methods include, among others steam reforming of natural gas [7], gasification of coal, biomass conversion [9,10], and electrolysis [11–13]. Special attention should be paid to electrolysis, whose main advantage is the possibility to produce hydrogen locally, right where it has to be used and no waste material is produced.

In the paper [4], a broad analysis of the possibilities for using hydrogen and fuel cells for heating is presented. Additionally, the problem of hydrogen distribution to households is discussed.

In the papers [14,15], the construction of PEM (proton exchange membrane) electrolyzers is described with the highlighted electrode construction and electrochemical processes taking place during the electrolysis process. In particular, the electrolysis process with electric and thermal energy requirements taken into account is described.

In the classical version, electrolysis is realized for an aqueous KOH (potassium hydroxide) solution [11,12] in electrolyzers fed from the source of direct current. However, in the papers [16–18], the results of experimental studies of the commercial alkaline electrolyzer

are presented. The authors of the paper [16] mainly focused on thermal problems. The considered electrolyzer is supplied by half-wave sinusoidal rectified current, the frequency of which is equal to approximately 160 Hz.

The information provided in [8] shows that electrolysis is not the most effective way to obtain hydrogen because the price of 1 kg is quite high; however, the use of hydrogen as an energy store in relatively simple and cheap photovoltaic installations allows for its storage in an effective way (compared to classic batteries). This can facilitate constant access to electrical energy in places without power grids and store surplus energy from the operation of power plants.

The paper [5] describes a system for power generation using photovoltaic systems, which includes electrolyzers that use the surplus of energy produced to generate hydrogen. This gas is an energy store in this system. In this case, the electrolyzer is powered by direct current. In turn, the paper [6] presents and analyzes the problem of supplying the electrolyzer with alternating voltage from the power grid.

Most water electrolysis systems use electrolyzers with a PEM membrane, which ensures better separation of gases (hydrogen and oxygen) and high energy efficiency [15,19,20]. However, the alkaline electrolyzers described, among others in the papers [20,21], are still of great importance.

For effective analysis of electrical and electronic networks and systems, mathematical models of all their components are necessary [22]. The more detailed the description of these components taking into account more physical phenomena, the more precise the analysis result is [23]. There are numerous models of electrolyzers in the literature. These models are described, inter alia, in the papers [19,20,24,25].

As a result of the papers [12,26], from the point of view of connectors, the electrolyzer can be treated as a non-linear RLC circuit. In compliance with Faraday's law, the mass of hydrogen produced is proportional to the value of the feeding current [12]. Additionally, the fact that ions occur with carriers of load in the solution is of essential importance. That is why the simultaneous transport of charge and mass occurs in the electrolyzer.

At a high value of current of the power supply, the efficiency of the process of hydrogen and oxygen production on the electrodes can be so high that it can cause a diminution of the effective area of the electrodes due to the occurrence of electro-hydrodynamic flows on these electrodes [27].

In the paper [28], a static and dynamic electrical model of the electrolyzer is proposed. This model identifies the value of the electrolyzer voltage as a function of current, temperature, and pressure. The cited paper shows the network representation of the proposed model, which consists of controlled voltage sources, capacitors, and a resistor. The correctness of the model was experimentally verified for the supply current frequency that was not higher than 100 Hz.

In the paper [14], the DC model of an electrolyzer, which allows computing voltage between the electrodes while considering the mass and charge transport, is presented. In turn, the electrode reaction process of the electrolyzer is described in the paper [29]. The stability of the electrode is also an important problem considered in the paper [30].

In turn, in the paper [31], the electrolyzer model dedicated to the MATLAB (MATrix LABoratory) program is proposed. The cited paper gives a mathematical description of the electrolyzer voltage–current characteristic, taking into account temperature and self-heating phenomena. The correctness of this model was experimentally verified. In the paper [32], the computed characteristics of the electrolyzer, which were obtained for selected values of temperature using the model published in the paper [31], are presented. The main subject of the paper [33] is also modeling the properties of the electrolyzer using the MATLAB program. The authors proposed a model that takes into account electrical, electrochemical, and thermodynamical phenomena. The correctness of this model was experimentally verified using a laboratory low-power electrolyzer.

In the paper [34], a lot of results of experimental findings illustrating the influence of frequency and the duty factor of the rectangular pulse train of voltage feeding the

electrolyzer on the waveforms of current of the electrolyzer and the power consumed from the power source are presented. In addition, in the cited paper, the measured dependences of the volume of the produced hydrogen on the feeding power while feeding the electrolyzer with DC voltage are presented. No conclusive analytical dependences on the considered quantities are formulated.

In the paper [17], the possibility of electrolysis at the power supply with the rectangular pulse train is considered. Problems connected with this process are discussed, and the possibility of using this type of power supply in practice is assessed.

In the authors' previous papers [26,35–38], the electrical model of an alkaline electrolyzer was proposed. This model has the form of a subcircuit for the SPICE (Simulation Program with Integrated Circuits Emphasis) software. Unfortunately, this model is very complicated and consists of diodes, resistors, inductors, and capacitors. However, diodes are semiconductor devices and they cannot exist in a real electrolyzer. By means of this model, a lot of computations are performed, showing that a change in the frequency of voltage feeding the electrolyzer can influence the current of the electrolyzer and the power received from the power source. The considered model has a behavioral character and it does not describe the relationship between the parameters describing the construction of the electrolyzer and the electrical properties of this device.

In [24], an alkaline electrolyzer model dedicated to the SPICE software was proposed. This model describes the static and dynamic properties of such an electrolyzer, but the effect of the solution concentration on the properties of this device was presented in a simplified manner, and the experimental verification was carried out in a narrow range of the electrolyzer supply current. The results of the verification of this model under dynamic operating conditions are not shown, either.

The paper [38] describes an in-built system dedicated to supplying an alkaline electrolyzer with a series of rectangular current pulse train of the adjustable frequency and the duty cycle. This paper presents exemplary results of the measurements of voltage and current waveforms of the electrolyzer under consideration.

The paper [39] contains an analysis of the usefulness of the W-Lambert function for modeling the current–voltage characteristics of an alkaline electrolyzer. It was shown in this paper that it is possible to obtain a good agreement between the calculated and measured characteristics  $i(v)$  for different values of the concentration of the solution, but it is necessary to use a very complex mathematical description.

As a result of the presented review of the literature, apart from the works of the authors, no one investigated the operation of the electrolyzer at the power supply of the pulsed signal at a frequency higher than 150 Hz. These investigations include mostly computer simulations.

This paper presents a method of modeling the DC (direct current) and dynamic characteristics of an alkaline electrolyzer. This method makes it possible to obtain a good agreement between the calculated and measured DC characteristics of such an electrolyzer and the dependence of the impedance of such an electrolyzer on frequency.

Section 2 describes the structure of the tested electrolyzer. Section 3 contains a description of the developed model. Section 4 presents the applied measurement systems. Section 5 shows and discusses the obtained results of calculations and measurements that illustrate the practical usefulness of the described model.

## 2. Tested Electrolyzer

The alkaline electrolyzer that is the subject of the paper was made by SESCO S.A. The view of the considered electrolyzer is shown in Figure 1.

It is made of stainless steel and it has the form of a roller with a volume equal to 10 l. On the opposite sides of this roller, there are connectors feeding the electrolyzer. Inside the electrolyzer, there are electrodes (anode and cathode) embedded in the insulating distance collars made of teflon. These electrodes have the shape of coaxial cylinders, and each of them contains a row of openings, making it possible to balance the level of the electrolyte.

Along each electrode, channels making it possible to take gases produced on the electrodes to separate reservoirs are situated [37].



**Figure 1.** View of the investigated alkaline electrolyzer.

The inside of the tested alkaline electrolyzer consists of two electrodes, designed in such a way as to maximize the surface, through which electric charges can move. Of course, the overall structure is relatively simple, which results in low production costs. The lower electrode (BOTTOM) consists of metal tubes stabilized with plastic mounting elements. The upper electrode (TOP) is made of cylindrical sheets which enter the spaces between the tubes mentioned above.

Two small, cylindrical tanks are designed to store the produced hydrogen and oxygen. The pressure gauge allows you to control the pressure of the gases produced. The valves allow for discharging the gases or replenishing the electrolyte.

### 3. Model Form

The electrolyzer model elaborated by the authors makes it possible to determine the DC current–voltage characteristics of the tested electrolyzer as well as the dependence of its impedance module on the frequency and dynamic characteristics of this device, taking into account changes in the electrolyte concentration. This model was formulated on the basis of the experimental results using splines and polynomials.

The DC current–voltage characteristics  $i(v)$  of the electrolyzer are described using the piecewise linear function of the form.

$$i = \begin{cases} 0 & \text{if } u < U_2 \\ \frac{v-U_2}{R_2} & \text{if } \frac{v-U_2}{R_2} > \frac{v-U_3}{R_3} \\ \frac{v-U_3}{R_3} & \text{if } \frac{v-U_3}{R_3} > \frac{v-U_1}{R_1} \\ \frac{v-U_1}{R_1} & \text{if } \frac{v-U_1}{R_1} > \frac{v-U_0}{R_0} \\ \frac{v-U_0}{R_0} & \text{if } \frac{v-U_1}{R_1} > \frac{v-U_0}{R_0} \end{cases} \quad (1)$$

In this formula, resistances  $R_0$ ,  $R_1$ ,  $R_2$ , and  $R_3$  characterize the slope of particular segments of the characteristics  $i(v)$ . The quotients  $U_i/R_i$  describe the intercepts in the equations describing the  $i$ -th part of the considered characteristics. All the coefficients in Formula (1) depend on the concentration of the electrolyte  $c$ . Based on the measurements of static characteristics, the coefficients in Formula (1) were determined for different values

of the electrolyte concentration. The following analytical relationships describing the influence of the electrolyte concentration on these coefficients are proposed:

$$U_0 = a_1 \cdot \exp\left(-\frac{c}{c_1}\right) + a_2 \cdot \exp\left(-\frac{c}{c_2}\right) + a_3 \quad (2)$$

$$U_1 = a_4 \cdot \exp\left(-\frac{c}{c_3}\right) + a_5 \quad (3)$$

$$U_2 = a_6 \cdot \exp\left(-\frac{c}{c_4}\right) + a_7 \cdot \exp\left(-\frac{c}{c_5}\right) + a_8 \quad (4)$$

$$U_3 = a_9 \cdot \exp\left(-\frac{c}{c_6}\right) + a_{10} \cdot \exp\left(-\frac{c}{c_7}\right) + a_{11} \quad (5)$$

$$R_0 = b_1 \cdot \exp\left(-\frac{c}{c_8}\right) + b_2 \cdot \exp\left(-\frac{c}{c_9}\right) + b_3 \quad (6)$$

$$R_1 = b_4 \cdot \exp\left(-\frac{c}{c_{10}}\right) - b_5 \cdot (c - c_{11})^2 + b_6 \quad (7)$$

$$R_2 = b_7 \cdot \exp\left(-\frac{c}{c_{12}}\right) + b_8 \quad (8)$$

$$R_3 = b_9 \cdot \exp\left(-\frac{c}{c_{13}}\right) + b_{10} \quad (9)$$

In Equations (2)–(9) parameters  $a_1, a_2, a_4, a_6, a_7, a_9,$  and  $a_{10}$  represent the coefficients in exponential dependences of voltages  $U_0, U_1, U_2,$  and  $U_3$  on concentration  $c$ . The slopes of the mentioned dependences describe the parameters  $c_1, c_2, c_3, c_4, c_5, c_6,$  and  $c_7$ . In turn, parameters  $a_3, a_5, a_8,$  and  $a_{11}$  are equal to the minimum values of voltages  $U_0, U_1, U_2,$  and  $U_3$ , respectively. Parameters  $b_1, b_2, b_4, b_7,$  and  $b_9$  represent the maximum changes in the values of resistances  $R_0, R_1, R_2,$  and  $R_3$  when changing the concentration of the electrolyte. Parameters  $c_8, c_9, c_{10}, c_{12},$  and  $c_{13}$  characterize the slope of the dependences of resistances  $R_0, R_1, R_2,$  and  $R_3$  on concentration  $c$ . The border values of resistances  $R_0, R_1, R_2,$  and  $R_3$  are represented by the parameters  $b_3, b_6, b_8,$  and  $b_9$ . Finally, parameters  $b_5$  and  $c_{11}$  describe the quadratic part of the dependence of resistance  $R_1$  on concentration  $c$ . Table 1 shows the values of the parameters occurring in Formulas (2)–(9). All the presented parameter values were estimated independently, but the values of some parameters are the same, e.g.,  $c_1, c_4, c_6, c_8,$  and  $c_{10}$ .

**Table 1.** Values of the parameters occurring in Formulas (2)–(9).

i	1	2	3	4	5	6	7	8	9	10	11	12	13
$a_i$ [V]	3.4	0.35	3.39	2	1.86	2.2	0.39	1.3	3.4	0.35	1.56	-	-
$b_i$ [Ω]	0.25	0.003	0.014	0.3	15	0.087	0.5	1	0.65	0.1	-	-	-
$c_i$ [-]	0.001	0.05	0.025	0.001	0.025	0.001	0.05	0.001	0.03	0.001	0.059	0.007	0.012

The rate of hydrogen production can be measured by the time  $t$  required to reach a certain pressure in the electrolyzer reservoir. This time depends on the value of the current  $i$  flowing through the electrolyzer and on the concentration of electrolyte  $c$ . In the developed model, the relationship  $t(i)$  is described by the formula:

$$t = A \cdot \exp\left(-\frac{i-F}{B}\right) + D \cdot \exp\left(-\frac{i}{E}\right) \quad (10)$$

where parameters  $A, B, D, E,$  and  $F$  depend on concentration  $c$  according to the following formulas.

$$A = A_0 - A_1 \cdot (c - A_2)^2 \quad (11)$$

$$B = B_0 + B_1 \cdot (c - B_2)^2 \quad (12)$$

$$D = D_0 - D_1 \cdot (c - D_2)^2 \quad (13)$$

$$E = E_0 \cdot \exp\left(-\frac{c}{E_1}\right) + E_2 + E_3 \cdot (c - E_4)^2 \quad (14)$$

$$F = F_0 - F_1 \cdot (c - F_2)^2 \quad (15)$$

Parameters  $A_0$ ,  $B_0$ ,  $D_0$ ,  $E_2$ , and  $F_0$  are the border values of parameters  $A$ ,  $B$ ,  $D$ ,  $E$ , and  $F$ , respectively. Parameter  $E_0$  represents the range of change in the exponential part of the dependence  $E(c)$ . The pairs of parameters  $A_1$  and  $A_2$ ,  $B_1$  and  $B_2$ ,  $D_1$  and  $D_2$ ,  $E_3$  and  $E_4$ , and  $F_1$  and  $F_2$  describe an influence of concentration  $c$  on the quadratic parts of dependences  $A(c)$ ,  $B(c)$ ,  $D(c)$ ,  $E(c)$ , and  $F(c)$ . Table 2 contains the parameter values of Formulas (11)–(15).

**Table 2.** Parameters values occurring in Formulas (11)–(15).

Parameter	$A_0$ [s]	$A_1$ [ks]	$A_2$	$B_0$ [A]	$B_1$ [A]	$B_2$	$D_0$ [s]	$D_1$ [ks]	$D_2$
value	2150	270	0.052	3.1	600	0.05	28	53	0.065
parameter	$E_0$ [A]	$E_1$	$E_2$ [A]	$E_3$ [A]	$E_4$	$F_0$ [A]	$F_1$ [A]	$F_2$	
value	28	0.0095	31	1400	0.05	2.05	150	0.035	

To describe the electrical dynamic properties of the electrolyzer operating without a DC power supply, its circuit analog was used in the form of a series connection of resistor  $R$ , capacitor  $C$ , and inductor  $L$ . The values of these elements depend on the concentration of the electrolyte using the following formulas.

$$C = C_0 \left(1 - \exp\left(-\frac{c - c_{C0}}{c_{C1}}\right)\right) + \frac{C_1}{C_2 + C_3 \cdot (c - c_{C2})^2} \quad (16)$$

$$R = R_0 + R_1 \cdot \exp\left(-\frac{c}{c_{R1}}\right) \quad (17)$$

$$L = L_0 - L_1 \cdot (c - c_{L1})^2 \quad (18)$$

Table 3 summarizes the values of the parameters occurring in Formulas (16)–(18).

**Table 3.** Values of the parameters occurring in Formulas (16)–(18).

Parameter	$C_0$ [mF]	$C_1$ [F]	$C_2$	$C_3$	$c_{C0}$	$c_{C1}$	$c_{C2}$
value	61	0.22	0.005	100	0.003	0.011	0.01
parameter	$R_0$ [mΩ]	$R_1$ [mΩ]	$c_{R1}$	$L_0$ [μH]	$L_1$ [H]	$c_{L1}$	
value	20	50	0.004	4.77	170	0.053	

As you can see, for the electrolyzer under consideration, the electrical capacity is several tens of millifarads, the resistance is tens of milliohms, and the inductance is a few microhenres.

#### 4. Measurement Set-Up

In order to verify the correctness of the electrolyzer model described in Section 3, measurements of the characteristics of the alkaline electrolyzer were carried out using the measuring setup shown in Figure 2.

In this setup, the DC power supply is connected in series with resistors and the tested electrolyzer. The electrolyzer is equipped with a barometer to measure the pressure of the produced gases. The voltmeter and the clamp ammeter enable measuring the coordinates of the electrolyzer operating point. The accuracy of the used voltmeter and ammeter is characterized by a relative error below 0.1%.

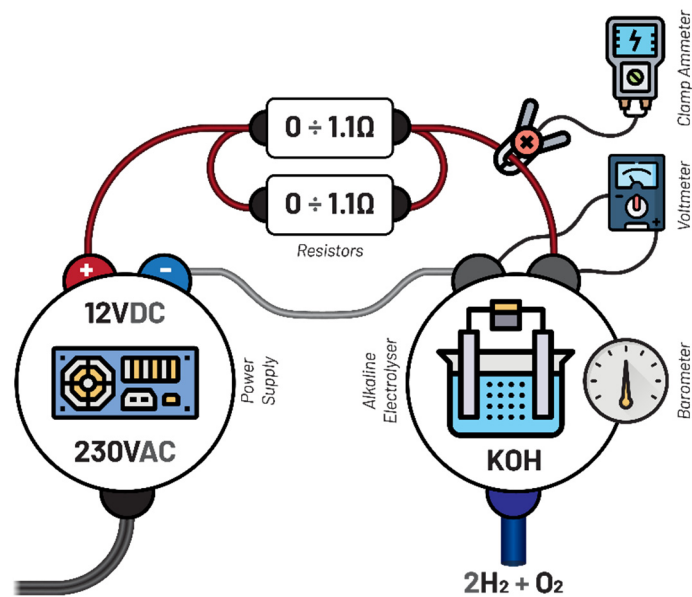


Figure 2. Setup for measuring electrolyzer characteristics.

While measuring the electrolyzer impedance, an automatic RLC bridge was used with the terminals to which the tested electrolyzer was connected. This bridge enables measurements to be made at selected frequency values ranging from 100 Hz to 200 kHz. The accuracy of the measurements performed by this RLC bridge is characterized by a relative error below 0.5%.

## 5. Measurement and Calculation Results

Using the measuring system described in Section 4, the characteristics of the tested electrolyzer were measured and compared with the results of the calculations obtained using the model described with the formulas given in Section 3. In the following figures, the results of the calculations are marked with lines, and the results of the measurements are marked with points.

Figure 3 shows the calculated and measured DC current–voltage characteristics  $i(v)$  of the tested electrolyzer filled with an electrolyte, which is an aqueous KOH solution of various concentrations  $c$ . The measurements carried out by the authors show that these characteristics exhibit central symmetry with respect to the point (0,0). Therefore, Figure 3 shows the course of these characteristics only for positive values of voltage  $v$ .

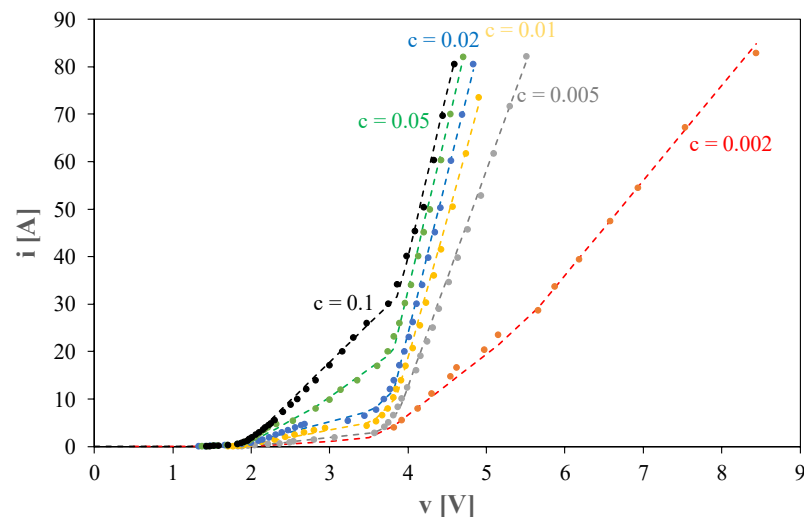
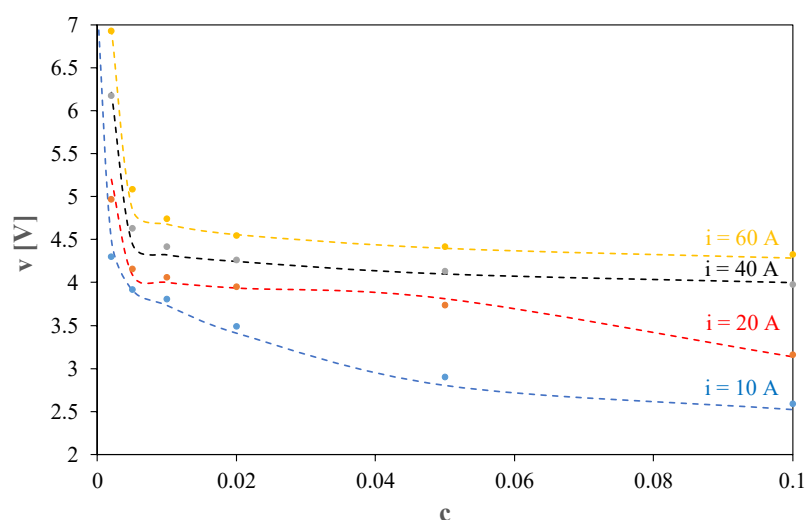


Figure 3. Calculated and measured DC current–voltage characteristics of the electrolyzer.

As can be seen, the relationship  $i(v)$  is a monotonically increasing function, and its course strongly depends on the value of the concentration of the electrolyte  $c$ . An increase in this concentration causes the characteristics to shift to the left. It can also be seen that an increase in the value of  $c$  causes a decrease in the value of the static resistance of the electrolyzer and a decrease in the voltage across the electrolyzer at a set value of the current flowing through it. For example, at  $i = 80$  A, voltage  $v$  decreases from 8.5 V at  $c = 0.002$  to just 4.1 V at  $c = 0.1$ . It is also worth noting that the slope of the characteristics  $i(v)$  increases with an increase in current  $i$ . The observed inflections of the dependence  $i(v)$  are a result of a change in the resistance of the electrolyte with changes in the electrolyte concentration. For all the considered characteristics, a good agreement between the calculation and measurement results was obtained.

Figure 4 shows the dependence of voltage  $v$  on the electrolyzer on the solution concentration  $c$  for selected values of current  $i$ .



**Figure 4.** Calculated and measured dependence of the electrolyzer voltage on the electrolyte concentration.

Figure 4 shows that the relationships  $v(c)$  for all the considered current values  $i$  are monotonically decreasing functions. The greatest changes in voltage are visible at low values of the concentration  $c$ . At the highest of the considered current values, a concentration change in the range from 0.02 to 0.1 causes almost imperceptible changes in voltage  $v$ . The slope of the dependence  $v(c)$  is very small in the range of high values of concentration  $c$ . Only for current  $i = 20$  A, this slope increases for the highest value of this concentration. The observed phenomena are thought of as changes in the resistivity of the electrolyte at different concentrations.

From the point of view of the user of the electrolyzer, the rate of hydrogen production is important. It can be expressed in the time  $t$  required to obtain a predetermined pressure in the electrolyzer. Figure 5 shows the dependence of time  $t$  required to obtain a pressure of  $0.2$  kg/cm<sup>2</sup> on the current supplied to the electrolyzer.

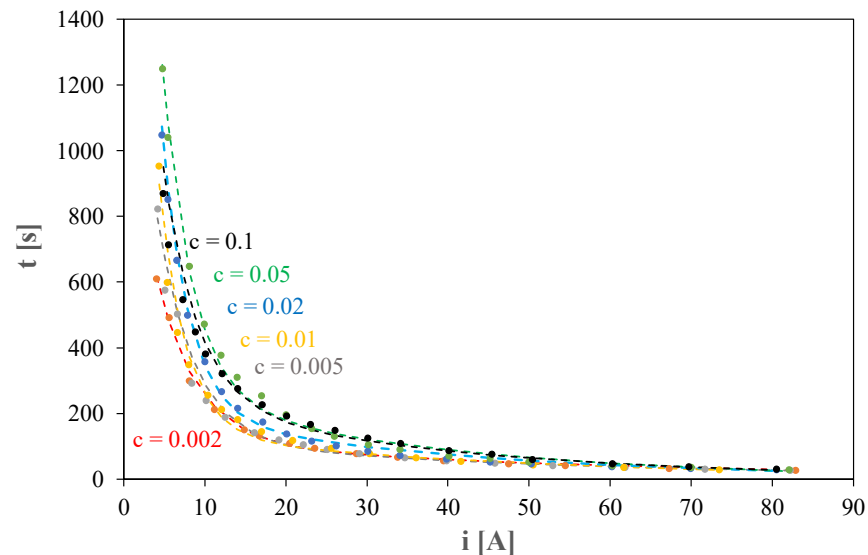
As can be seen, the considered dependence is a monotonically decreasing function. With changes in the current value from 4 to 80 A, time  $t$  decreases from 1300 s to only 30 s. A particularly significant reduction in time  $t$  is visible in the range of low current values. It may be surprising that at low current values and an increase in the electrolyte concentration, time  $t$  even doubles.

Figure 6 shows the dependence of time  $t$  on the electrolyte concentration  $c$  for selected values of current  $i$ . The absolute error of the measurement of time is equal to 1 s and the calculated values of time were obtained using Equations (10)–(15).

As can be seen, the concentration of the electrolyte strongly influences time  $t$ . For example, at current  $i = 10$  A, these changes are more than twofold. It is worth noting that for the lower of the considered current values  $i$ , the relationship  $t(c)$  has a maximum at



$c = 0.05$ . For high current values, the considered dependence is an increasing function. On the other hand, for a set value of  $c = 0.05$ , an increase in the current value from 10 A to 60 A causes a 10-fold decrease in the value of time  $t$ . In turn, at high values of current, the changes in the values of time are poorly visible due to big differences between the values of time obtained for different current values. For the highest of the considered values of current, the changes in the values of time exceed even 30%.



**Figure 5.** Calculated and measured dependence of time  $t$  on the electrolyzer supply current.

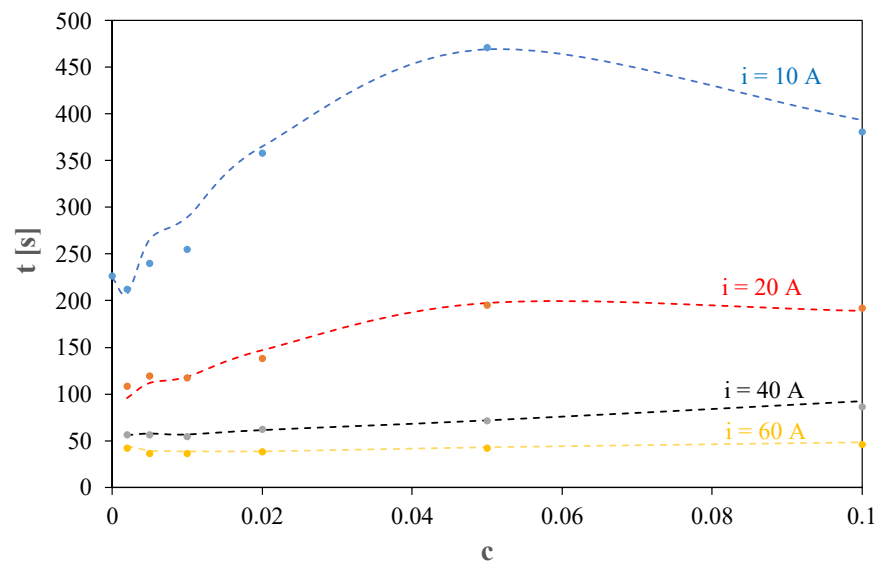


**Figure 6.** Calculated and measured dependence of time  $t$  on the electrolyte concentration.

By analyzing Figure 6, it can be concluded that the highest hydrogen generation rate is obtained at a concentration of  $c = 0.01$  for high values of current. At lower values of current, the productivity of the electrolyzer is better at lower values of the electrolyte concentration. However, as can be seen from Figure 3, the lower the concentration value  $c$ , the higher the voltage  $v$  across the electrolyzer. In order to illustrate the relationship between the rate of hydrogen generation and the power delivered to the electrolyzer, Figure 7 presents the dependence of the time ratio  $t$  by power  $p$  on the electrolyte concentration for selected values of power  $p$  dissipated in the electrolyzer.

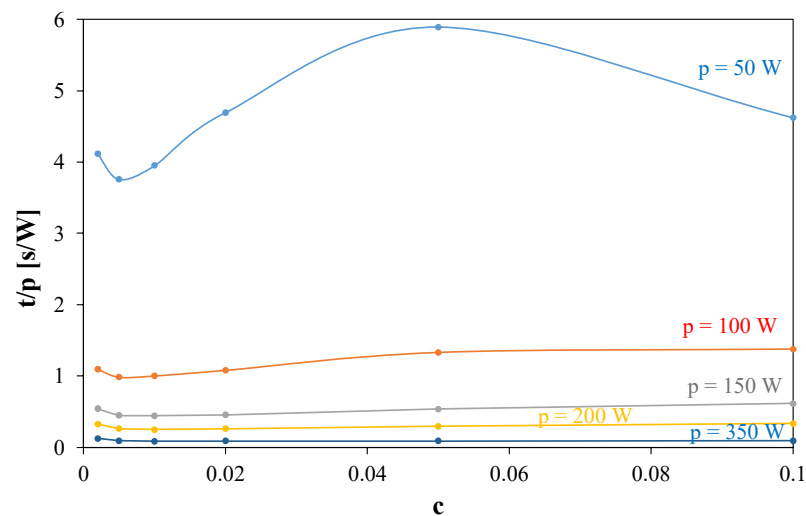


**Figure 7.** Calculated and measured dependence of the time ratio  $t$  by power  $p$  on the electrolyte concentration for selected values of power  $p$  dissipated in the electrolyzer.

As can be seen, the most favorable operating conditions, i.e., the lowest value of the  $t/p$  ratio, are obtained for the highest of the considered values of power  $p$  and at concentration  $c = 0.01$ . Thus, it is not preferable to use too high a concentration of the solution as this entails a greater cost of potassium hydroxide to be used and a decrease in the productivity of the electrolyzer.

The results presented above refer to the operation of the electrolyzer in DC conditions, i.e., when supplied with direct current. However, this device is also capable of operating on an AC power supply. Therefore, its dynamic parameters are important. Figure 8 shows the dependence of the impedance module of the tested electrolyzer on the frequency for selected solution concentration values.

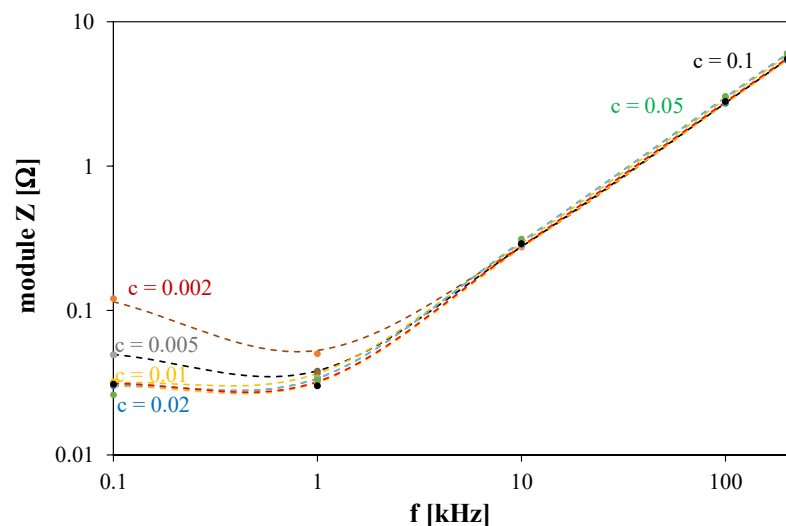


**Figure 8.** Calculated and measured dependence of the electrolyzer impedance module on frequency.

The considered dependence has a minimum at frequency  $f = 1$  kHz. As concentration  $c$  increases, the value of the impedance modulus decreases at low frequencies. It can be seen from the shape of the obtained dependence that in the range of low frequency, the impedance of the electrolyzer is capacitive, and in the range of high frequencies, it is inductive.

Figures 9 and 10 illustrate the dependence of the capacitance  $C$  of the electrolyzer and its inductance  $L$  on the concentration of the solution. The electrolyzer resistance was

also determined and its value was about 20 m $\Omega$ . It is related to the resistance of the electrolyzer electrodes.

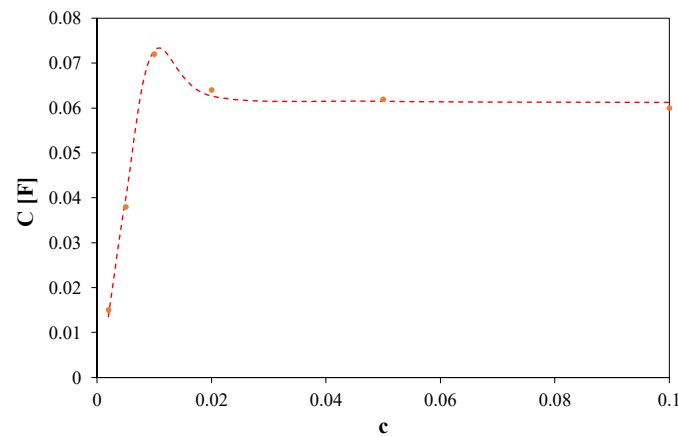


**Figure 9.** Calculated and measured dependencies of the electrolyzer electric capacity on the electrolyte concentration.

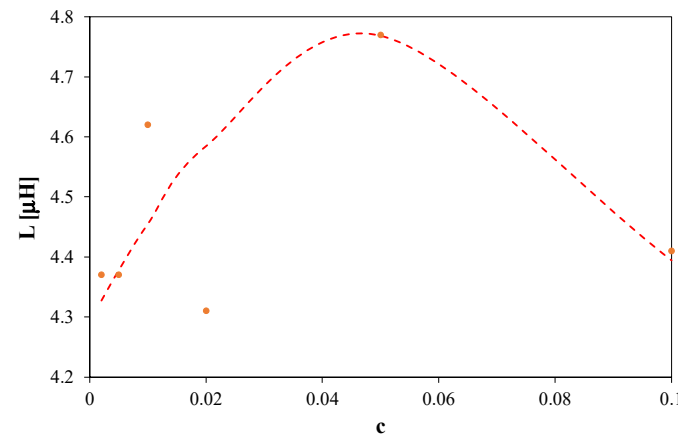


**Figure 10.** Calculated and measured dependencies of the electrolyzer inductance on the electrolyte concentration.

As can be seen in Figure 9, the electric capacity of the electrolyzer takes higher values ranging from 15 to 75 mF. The maximum of the relationship  $C(c)$  occurs at a concentration of  $c = 0.01$ . For high concentration values ( $c > 0.02$ ), the capacity of the electrolyzer practically does not depend on the concentration of the solution.

In turn, from Figure 10, it can be seen that the inductance of the electrolyzer changes by only 10% with the variation of the electrolyte concentration within the considered limits. The maximum inductance occurs at  $c = 0.05$ . Inductance  $L$  is mainly related to the leads and electrodes of the electrolyzer. A change in the inductance value can be a result of a change in the reactance of the electrolyte with an increase in its concentration.

The obtained values of inductance and capacitance of the electrolyzer make it practically impossible for the considered electrolyzer to be fed effectively with the use of a rectangular voltage pulse train, which was considered in [38]. With such a supply, the voltage on the electrolyzer changes in a narrow range and does not reach zero after switching off, while the current has the shape of an exponential wave.

## 6. Conclusions

This paper describes the results of the investigations concerning the properties of an alkaline electrolyzer. A description of the tested electrolyzer was presented, and the model of this electrolyzer was proposed in the form of a set of equations describing its current–voltage characteristics, the dependence of the time needed to produce a given

value of hydrogen on the supply current. In each of these relationships, the effect of the electrolyte concentration was taken into account. The influence of the concentration of the electrolyte on the values of the RLC elements in the network analog of the electrolyzer is also described.

The form of the proposed model is universal, and it can also be used for other electrolyzers, but the values of the coefficients given in this article are specific to the tested electrolyzer. This model was verified only for the one electrolyzer described in this article.

The performed calculations and measurements showed that the concentration of the electrolyte strongly influences the course of the characteristics  $i(v)$  and  $t(i)$ , as well as the values of the RLC elements. Changes in the course of the above-mentioned characteristics and the values of RLC elements are particularly clear at low values of the electrolyte concentration  $c \leq 0.01$ . At high values of the electrolyte concentration, these changes slightly affect the characteristics of the electrolyzer. It may be related to reaching electrolyte saturation concentration.

The comparison of the results of calculations and measurements confirmed that the electrolyzer model proposed in this paper allows for the correct description of its DC and dynamic characteristics. The correctness of the model was demonstrated in a wide range of changes in the solution concentration, supply current, and frequency. In the performed investigations, the energy balance of the electrolyzer and the heat loss distribution were not considered. Taking into account the mentioned phenomena, the accuracy of the presented model can be improved.

The presented research results may be useful for designers of hydrogen production systems using water electrolysis. They can also be useful for designers of energy storage systems cooperating with renewable energy sources. The proposed model can be used to optimize the concentration of the electrolyte, at which the productivity of the electrolyzer is the most profitable and the consumed electrical power is acceptable.

The obtained results of the investigations show that the operation of the considered electrolyzer is possible with the power supply from a DC source or a source of a current pulse train of a low-frequency value. Due to the high value of the electrolyzer capacitance, it is not possible to change the value of the electrolyzer current quickly. From the experiments performed by us for the tested electrolyzer, the frequency of operation should be no higher than 100 Hz.

The presented investigations were performed for the electrolyzer containing a KOH electrolyte only. In further investigations, other electrolytes will also be considered. The next direction of our investigation will be modeling the properties of electrolyzers operating at the power supply by a voltage rectangular pulse train of different frequency values.

**Author Contributions:** Conceptualization, K.G.; methodology, K.G. and P.G.; validation, K.G.; investigation, E.Ś. and K.G.; writing—original draft preparation, K.G. and P.G.; writing—review and editing, K.G., P.G. and E.Ś.; visualization, K.G. and E.Ś.; supervision, K.G. All authors have read and agreed to the published version of the manuscript.

**Funding:** The project is financed within the program of the Ministry of Science and Higher Education called “Regionalna Inicjatywa Doskonałości” in the years 2019–2023, under project number 006/RID/2018/19, with a sum of financing of 11 870 000 PLN.

**Data Availability Statement:** Data available for request.

**Conflicts of Interest:** The authors declare no conflict of interest.

## References

1. Hillmansen, S. Hydrogen and its role in railway decarbonisation. Keynote speech. In Proceedings of the 16th International Conference on Compatibility, Power Electronics and Power Engineering IEEE CPE-POWERENG 2022, Birmingham, UK, 29 June–1 July 2022.
2. Breeze, P. *Power System Energy Storage Technologies*; Elsevier: Amsterdam, The Netherlands, 2018.

3. Cutululis, N.A. Wind power as the backbone of the decarbonized energy systems. Keynote speech. In Proceedings of the 16th International Conference on Compatibility, Power Electronics and Power Engineering IEEE CPE-POWERENG, Birmingham, UK, 29 June–1 July 2022.
4. Dodds, P.E.; Staffell, I.; Hawkes, A.D.; Li, F.; Grunewald, P.; McDowall, W.; Ekins, P. Hydrogen and fuel cell technologies for heating: A review. *Int. J. Hydrogen Energy* **2015**, *40*, 2065–2083. [CrossRef]
5. Toghyani, S.; Afshari, E.; Baniasadi, E.; Shadloo, M. Energy and exergy analyses of a nanofluid based solar cooling and hydrogen production combined system. *Renew. Energy* **2019**, *141*, 1013–1025. [CrossRef]
6. Ursúa, A.; Marroyo, L.; Gubía, E.; Gandía, L.M.; Diéguez, P.M.; Sanchis, P. Influence of the power supply on the energy efficiency of an alkaline water electrolyser. *Int. J. Hydrogen Energy* **2009**, *4*, 3221–3233. [CrossRef]
7. Mizeraczyk, J.; Urashima, K.; Jasinski, M.; Dors, M. Hydrogen Production from Gaseous Fuels by Plasmas—A Review. *Int. J. Plasma Environ. Sci. Technol.* **2014**, *8*, 89–97.
8. Nikolaidis, P.; Poullikkas, A. A comparative overview of hydrogen production processes. *Renew. Sustain. Energy Rev.* **2017**, *67*, 597–611. [CrossRef]
9. Cortright, R.D.; Davda, R.R.; Dumesic, J.A. Hydrogen from catalytic reforming of biomass-derived hydrocarbons in liquid water. *Nature* **2002**, *418*, 964–967. [CrossRef] [PubMed]
10. Obiecuja Metoda Produkcji Wodoru. Available online: <http://kopalniawiedzy.pl/wodor-ksyloza-zrodla-odnawialnebiopaliwo,17845> (accessed on 25 September 2022).
11. Mazloomi, K.; Sulaiman, N.; Ahmad, S.A.; Yunus, N.A. Analysis of the Frequency Response of a Water Electrolysis Cell. *Int. J. Electrochem. Sci.* **2013**, *8*, 3731–3739.
12. Mazloomi, K.; Sulaiman, N.; Moayedi, H. An Investigation into the Electrical Impedance of Water Electrolysis Cells—With a View to Saving Energy. *Int. J. Electrochem. Sci.* **2012**, *7*, 3466–3481.
13. Randolph, K. Hydrogen production—Session introduction. In Proceedings of the 2013 Annual Merit Review and Peer Evaluation Meeting, Arlington, VA, USA, 16 May 2013.
14. Carmo, M.; Fritz, D.L.; Mergel, J.; Stolten, D. A comprehensive review on PEM water electrolysis. *Int. J. Hydrogen Energy* **2013**, *38*, 4901–4934. [CrossRef]
15. Zhang, K.; Liang, X.; Wang, L.; Sun, K.; Wang, Y.; Xie, Z.; Wu, Q.; Bai, X.; Hamdy, M.S.; Chen, H.; et al. Status and perspectives of key materials for PEM electrolyzer. *Nano Res. Energy* **2022**. [CrossRef]
16. Diéguez, M.P.M.; Ursúa, A.; Sanchis, P.; Sopena, C.; Guelbenzu, E.; Gandía, L.M. Thermal performance of a commercial alkaline water electrolyzer: Experimental study and mathematical modeling. *Int. J. Hydrogen Energy* **2008**, *33*, 7338–7354. [CrossRef]
17. Monk, N.; Watson, S. Review of pulsed power for efficient hydrogen production. *Int. J. Hydrogen Energy* **2016**, *41*, 7782–7791. [CrossRef]
18. Artuso, P.; Gammon, R.; Orecchini, F.; Watson, S.J. Alkaline electrolyzers: Model and real data analysis. *Int. J. Hydrogen Energy* **2011**, *36*, 7956–7962. [CrossRef]
19. Hernández-Gómez, Á.; Ramirez, V.; Guilbert, D.; Saldivar, B. Cell voltage static-dynamic modeling of a PEM electrolyzer based on adaptive parameters: Development and experimental validation. *Renew. Energy* **2020**, *163*, 1508–1522. [CrossRef]
20. Estejab, A.; Daramola, D.A.; Botte, G.G. Mathematical model of a parallel plate ammonia electrolyzer for combined wastewater remediation and hydrogen production. *Water Res.* **2015**, *77*, 133–145. [CrossRef]
21. Henaou, C.; Agbossou, K.; Hammoudi, M.; Dubé, Y.; Cardenas, A. Simulation tool based on a physics model and an electrical analogy for an alkaline electrolyser. *J. Power Sources* **2014**, *250*, 58–67. [CrossRef]
22. Rashid, M.H. *SPICE for Power Electronics and Electric Power*; CRC Press: Boca Raton, FL, USA, 2017.
23. Górecki, P.; Górecki, K. Methods of Fast Analysis of DC-DC Converters—A Review. *Electronics* **2021**, *10*, 2920. [CrossRef]
24. Górecki, K.; Górecka, M.; Górecki, P. Modelling properties of an alkaline electrolyser. *Energies* **2020**, *13*, 3073. [CrossRef]
25. Ursúa, A.; Sanchis, P. Static-dynamic modelling of the electrical behaviour of a commercial advanced alkaline water electrolyser. *Int. J. Hydrogen Energy* **2012**, *37*, 18598–18614. [CrossRef]
26. Górecki, K.; Zarębski, J.; Górecki, P.; Halbryt, S. Modelling and the analysis of the power supply system for the generator of hydrogen. In *Proceedings of the 2nd International Congress on Energy Efficiency and Energy Related Materials (ENEFM2014), Fethiye, Turkey, 16–19 October 2014*; Springer Proceedings in Energy; Springer: Berlin/Heidelberg, Germany, 2015; pp. 112–118.
27. Podliński, J.; Niewulis, A.; Mizeraczyk, J. Electrohydrodynamic flow and particle collection efficiency of a spike-plate type electrostatic precipitator. *J. Electrostat.* **2009**, *67*, 99–104. [CrossRef]
28. Dobo, Z.; Palotas, A.B. Impact of the current fluctuation on the efficiency of alkaline water electrolyser. *Int. J. Hydrogen Energy* **2017**, *41*, 5627–6434.
29. Gao, F.; He, J.; Wang, H.; Lin, J.; Chen, R.; Yi, K.; Huang, F.; Lin, Z.; Wang, M. Te-mediated electro-driven oxygen evolution reaction. *Nano Res. Energy* **2022**. [CrossRef]
30. Zhang, L.; Liang, J.; Yue, L.; Dong, K.; Li, J.; Zhao, D.; Li, Z.; Sun, S.; Luo, Y.; Liu, Q.; et al. Benzoate anions-intercalated NiFe-layered double hydroxide nanosheet array with enhanced stability for electrochemical seawater oxidation. *Nano Res. Energy* **2022**. [CrossRef]
31. Ulleberg, Ø. Modeling of advanced alkaline electrolyzers: A system simulation approach. *International Journal of Hydrogen Energy* **2003**, *28*, 21–33. [CrossRef]

32. Tijani, A.S.; Yusup, N.A.B.; Rahim, A.H.A. Mathematical modelling and simulation analysis of advanced alkaline electrolyzer system for hydrogen production. *Procedia Technol.* **2014**, *15*, 798–806. [[CrossRef](#)]
33. Agbli, K.S.; Péra, M.C.; Hissel, D.; Rallières, O.; Turpin, C.; Doumbia, I. Multiphysics simulation of a PEM electrolyser: Energetic Macroscopic Representation approach. *Int. J. Hydrogen Energy* **2011**, *36*, 1382–1398. [[CrossRef](#)]
34. Shaaban, A.H. Pulsed DC and Anode Depolarization in Water Electrolysis for Hydrogen Generation, Report ESL-TR-92-55. 1994. Available online: <https://apps.dtic.mil/dtic/tr/fulltext/u2/a297375.pdf> (accessed on 25 September 2022).
35. Górecki, P.; Górecki, K. The influence of a mounting manner of power MOS transistors on characteristics of the Totem-Pole circuit with RLC load. *Microelectron. Int.* **2016**, *33*, 176–180. [[CrossRef](#)]
36. Górecki, P.; Górecki, K.; Zarebski, J. Modelowanie właściwości elektrolizera w programie SPICE. *Elektronika* **2017**, *10*, 15–18. [[CrossRef](#)]
37. Górecki, K.; Górecki, P.; Zarebski, J. Electrical model of the alkaline electrolyser dedicated for SPICE. *Int. J. Circuit Theory Appl.* **2018**, *46*, 1044–1054. [[CrossRef](#)]
38. Świtalski, E.; Górecki, K. System wbudowany do badania właściwości elektrolizera. *Przegląd Elektrotechniczny* **2022**, *98*, 151–154. [[CrossRef](#)]
39. Świtalski, E.; Górecki, K. Wykorzystanie funkcji W-Lamberta do modelowania charakterystyk elektrolizera alkalicznego. *Przegląd Elektrotechniczny* **2022**, *98*, 150–153. [[CrossRef](#)]